PHYSICAL REVIEW E **77**, 055101(R) (2008)

Optically driven nonlinear microrheology of gelatin

James N. Wilking[1] and Thomas G. Mason[1,2,*]

[1]*Department of Chemistry and Biochemistry, University of California-Los Angeles, Los Angeles, California 90095, USA*

[2]*Department of Physics and Astronomy, and California NanoSystems Institute, University of California-Los Angeles, Los Angeles, California 90095, USA*

(Received 13 December 2007; published 6 May 2008)

We demonstrate the microscopic equivalent of a step-stress rheological measurement. An optical torque is applied to a birefringent wax microdisk embedded in gelatin, a highly entangled viscoelastic biopolymer, using circularly polarized laser tweezers. By increasing the laser power and measuring the angular displacement of the disk, we explore the microscopic rheological response of presheared gelatin from the linear to the nonlinear regime and observe yielding at the microscale. The shape of the microscopic torque-angle relationship matches the stress-strain relationship from a macroscopic measurement of presheared gelatin; from this, we extract an applied stress and deduce the effective strain induced by the rotating disk.

DOI: 10.1103/PhysRevE.77.055101 PACS number(s): 83.60.La, 83.60.Rs, 83.80.Lz, 87.80.Cc

Microrheology encompasses the study of deformation and flow of soft materials [1,2] at microscopic and smaller length scales. Thermal microrheology [3,4] is a useful method for deducing the local *linear* viscoelasticity of a soft material from the equilibrium thermal fluctuations of colloidal probe particles in it. If the material is homogeneous, its bulk viscoelastic moduli can also be inferred through the generalized Stokes-Einstein relation [3]. Because thermal microrheology is based on equilibrium dynamics, it is unsuitable for probing local nonlinear rheology. To go beyond the linear regime, actively driven microrheology techniques are necessary.

Optical tweezers or magnetic field gradients [5–7] can be coupled to microscopic probes to produce stresses that far exceed those created by thermal energy. To date, there are only a few studies of the nonlinear microrheology of soft complex materials [8–12]. The linear and nonlinear steady-shear viscosities of wormlike micelle solutions have been investigated using a magnetically driven rotating nanowire [10], and the linear and nonlinear drag forces on magnetically driven [11] and optically trapped [12] microspheres have been studied as they are translated through dense colloidal suspensions. Although these measurements have focused primarily on linear and nonlinear steady-shear viscosities of soft viscoelastic materials, no observation of "yielding" at the microscale has been reported, with emphasis on local departure from Hookean behavior.

Here, we use a microscopic apparatus that is analogous to a controlled stress rheometer to apply stresses large enough to observe yielding of a soft biomaterial at the microscale. We embed birefringent colloidal microdisks in a viscoelastic biopolymer gelatin, reorient a disk in a highly focused laser trap using torques induced by the circular polarization of the laser light, and measure the corresponding angular displacement of the disk. By systematically increasing the laser power, we increase the local applied stress and ultimately observe yielding of the gelatin at the microscale.

We create birefringent wax microdisks by emulsifying hot α-eicosene wax, which melts at 26 °C, in an aqueous sodium dodecyl sulfate (SDS) solution ($1M$) at 70 °C, cooling to 23 °C and annealing for several months. This method [13] produces disks with a large distribution in radii, $0.2\ \mu\text{m} < a < 10\ \mu\text{m}$, and aspect ratio, $2 \leq (2a)/h \leq 10$, where h is the thickness of the disk. Herein, we use a disk with an aspect ratio of $(2a)/h \approx 2$.

We prepare sealed samples of microdisks at a dilute volume fraction, ϕ, in gelatin, a biopolymer obtained from the partial hydrolysis of collagen [14]. The individual polypeptide chains in gelatin interact noncovalently, naturally forming triple helices as the principal structural motif. These structures are disrupted at elevated temperatures, and gelatin is easily dissolved in hot water, existing as statistically random polymer coils. If the gelatin concentration is great enough so that individual chains overlap (0.4% to 1.0%) [14], upon cooling, intermolecular and intramolecular triple helices will form and the entangled polymer will form a gel. The degree of helix formation and density of physically entangled helical cross links are concentration and history dependent; sensitive both to the annealing temperature and time. For our experiment, an aqueous solution of gelatin (type B, $\text{MW} \approx 10^4 - 10^5$, 1.5% w/w) was dissolved at 80 °C and allowed to cool to room temperature before the addition of microdisks at $\phi \approx 10^{-5}$. The viscous solution was then sealed in a glass microscope cell for optical trapping studies, and gelation was induced at 15 °C for 12 h. The remainder of the sample was used in bulk rheology measurements. Scattering [15] and electron microscopy [16] performed on aqueous gelatin gels of similar molecular weight and at comparable concentrations have shown that the gel is well entangled, with a characteristic entanglement length $10\ \text{nm} \leq \xi \leq 100\ \text{nm}$, significantly smaller than the length scale of the probe particles.

A single-beam optical trap [17,18] with polarization and shutter control is used for manipulating the microdisks [13] [Fig. 1(a)]. A high-powered laser is focused by a microscope objective to a symmetric diffraction-limited spot within the gelatin sample [Fig. 1(b)]. Thin wax microdisks have previously been shown to trap "on edge" [13,19] in the spot; the disk's symmetry axis aligns perpendicular to the optical axis. Linearly polarized (LP) laser light is converted into circu-

*Author to whom correspondence should be addressed. mason@physics.ucla.edu

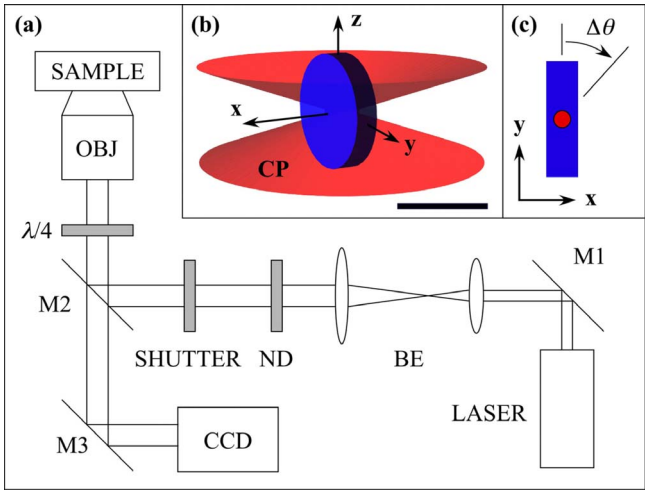

FIG. 1. (Color online) (a) Schematic of the optical trapping apparatus. A krypton ion laser ($P_{MAX} \approx 1.5$ W, $\lambda = 647$ nm, LP) is directed with mirrors (M1, dichroic M2) through a beam expander (BE, 5X) into the back aperture of a microscope objective (OBJ, Nikon 100X Plan Apo, NA=1.4) and focused to a diffraction limited spot within the sample. The laser intensity is controlled with neutral density filters (ND) and a computer controlled shutter. The introduction of a quarter wave plate ($\lambda/4$) circularly polarizes (CP) the laser light. A CCD camera images the sample. (b) A wax microdisk (blue) traps upright in the diffraction limited optical trap (red). The scale bar is 2 μm. (c) CP laser light applies a torque to the birefringent microdisk resulting in an angular displacement, $\Delta\theta$ about the optical axis (red circle).

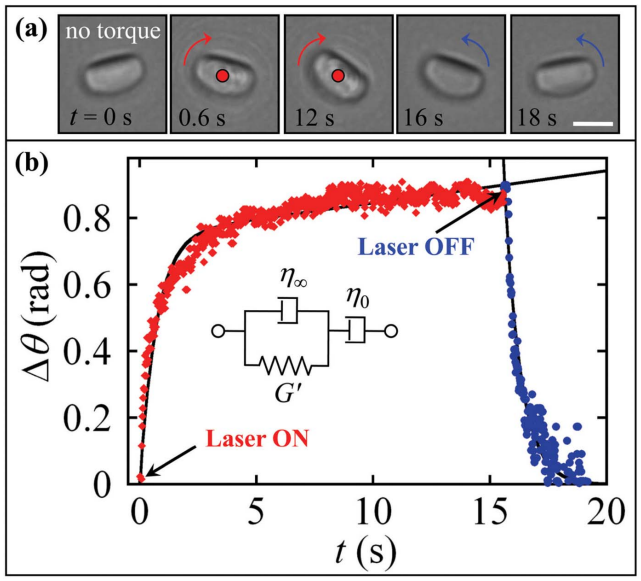

FIG. 2. (Color online) (a) A wax microdisk [$a \approx 1.5$ μm, $(2a)/h \approx 2$] embedded in an aqueous gel (gelatin, 1.5% w/w) is viewed on edge ($t=0$ s). The application of an optical torque ($P=1$ W, $t=0.6$ s and 12 s) rotates the disk CW (red arrows) about the optical axis (red circles); upon removal of the torque ($t=16$ s and 18 s), the disk rotates CCW (blue arrows) to its original position. The scale bar is 2 μm. (b) The time-dependent angular response $\Delta\theta(t)$ of the microdisk to an applied torque ("Laser ON," red diamonds) is fit to a simple model for the strain response of a viscoelastic material subjected to a step stress (schematic, inset). The angular relaxation of the disk ("Laser OFF," blue circles) is fit to a simple exponential decay.

larly polarized (CP) light by introducing a quarter wave plate ($\lambda/4$); the CP light exerts a unidirectional torque T on the birefringent microdisk [Fig. 1(c)] due to a change in angular momentum as it traverses the disk. Due to T, the disk rotates about the optical axis from its initial angle at rest to an angle $\Delta\theta$. For an axially symmetric trap, T is independent of $\Delta\theta$, and the clockwise (CW) or counterclockwise (CCW) direction of T can be selected by the handedness of the CP light. No significant heating of the disk by the absorption of laser light is observed at all laser powers we use. Due to the relatively low melting point of the wax, even a slight increase in temperature would have resulted in a dramatic change of the probe's shape. The disk is illuminated using a brightfield condenser; the dichroic mirror below the objective permits the orientation of the disk to be imaged at 60 fps using a color charge-coupled device (CCD) camera without leakage from backscattered laser light. We calibrate T applied to a microdisk by measuring its rotational frequency f in water over a wide range in laser power, $10\ \text{mW} \leq P \leq 500\ \text{mW}$. From $f(P)$ we determine the Stokes drag torque, T_d, for a thin disk that is spinning on edge: $T_d = (32/3)\eta a^3 \omega$ [20], where η is the viscosity of water and $\omega = 2\pi f$ is its angular frequency. From $T_d(P)$ we obtain a slope of $2.62 \pm 0.07 \times 10^{-13}$ dyn cm/mW.

We conduct microrheological step-stress measurements at 23 °C on a microdisk suspended in the gelatin. A disk located 10 ± 0.5 μm from the coverglass surface is brought into alignment with the trap's optical axis using the microscope stage. To facilitate measurements of $\Delta\theta$, we initially orient the disk "on edge" without spinning it by subjecting it to a low-power ($P \approx 10$ mW) randomly polarized (RP) laser trap for 10 minutes using a depolarizing filter. This step effectively preshears the gelatin around the disk. We block the laser using the shutter for several minutes and verify proper alignment of the disk; absence of residual stresses in the gel is confirmed by minimal drift. By rapidly opening the shutter, we subject the disk to a step-stress using a CP optical trap at a specific P. After a fixed period of time, the shutter is closed, and creep recovery is observed. When repeatedly applying step stresses to the same disk, the surrounding gel is allowed to equilibrate for several minutes between each measurement while the laser is blocked. The time-dependent angular displacement $\Delta\theta(t)$ of the microdisk is determined from video tracking of the disk's profile. Since the size and aspect ratio of the disk chosen closely matches the one used in the calibration, T can be accurately calculated. For comparison, the bulk stress-strain relationship of the same gelatin sample is measured at 23 °C using a controlled-strain rheometer (25 mm diameter cone and plate). When the upper cone is lowered, the gel is presheared. Oscillatory strain sweep measurements at 1 rad/s are performed to determine the yield stress and strain of the gelatin.

A representative microscopic step-stress and recovery measurement is shown in Fig. 2(a). After T is applied, the disk rapidly rotates CW about the optical axis and then nearly stops; $\Delta\theta$ increases very slowly thereafter. Following

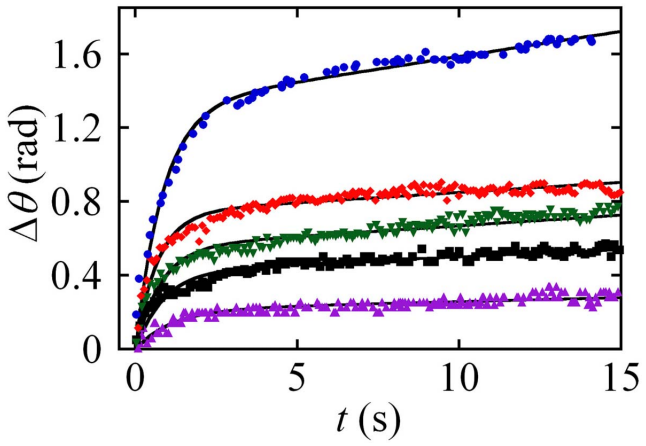

FIG. 3. (Color online) The angular displacement $\Delta\theta(t)$ of the microdisk (from Fig. 2) as a function of increasing laser power, P =270 (▲) (purple online), 600 (■) (black online), 800 (▼) (green online), 1000 (♦) (red online), and 1500 mW (●) (blue online). The lines are fits to a model of a viscoelastic material subjected to a step stress [see Fig. 2(b) (inset)].

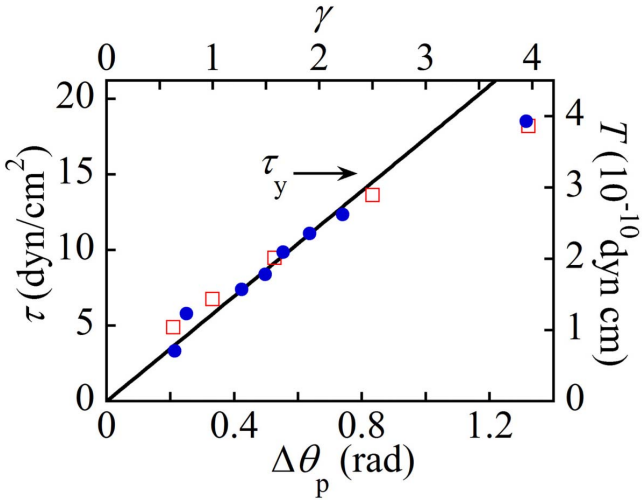

FIG. 4. (Color online) Bulk rheology of presheared gelatin (□) (red online), plotted as the macroscopic stress τ (left axis) versus macroscopic strain, γ (upper axis), exhibiting a yield stress, $\tau_y \approx 15 \pm 3$ dynes/cm^2. Optical torque, T (right axis) applied to a wax microdisk (from Fig. 2) embedded in gelatin versus the angular displacement $\Delta\theta_p$ (lower axis) of the disk (●) (blue online). The line is a linear fit to the data below $T \approx 3 \times 10^{-10}$ dyn cm. Data at $T \approx 3.9 \times 10^{-10}$ dyn cm deviate significantly from linearity. The relative scales of the horizontal and vertical axes have been adjusted to provide the best agreement between the macroscopic and microscopic rheology.

the application of the step stress, the disk's angular displacement rises nearly exponentially with time to an apparent plateau $\Delta\theta_p$. The positive slope of the saturation plateau indicates a low frequency relaxation of the polymer network under the applied stress. When the laser is blocked, the disk rotates CCW due to the restoring torque from the stretched polymers around it and returns to its original orientation, within our resolution [Fig. 2(b)].

The microdisk's response can be modeled by a Kelvin-Voigt element [i.e., elastic spring with modulus G' and dashpot with high frequency viscosity η_∞ in parallel] in series with a dashpot representing a low frequency viscosity η_0 [see Fig. 2(b), inset] [1]. Correspondingly, the data are fit by $\Delta\theta(t) = \Delta\theta_p\{[1-\exp(-t/t_\infty)] + (t/t_0)\}$, where $t_\infty = \eta_\infty/G'$ is the high-frequency relaxation time, $t_0 = \eta_0/G'$ is the low-frequency relaxation time, and $\Delta\theta_p$ is the plateau angular displacement. For small stresses, theory predicts $\Delta\theta_p$ to be proportional to T and inversely proportional to G'. This model provides a reasonable fit [Fig. 2(b)]. When the optical stress is removed, the disk's return to its original orientation is fit well by a simple exponential decay: $\Delta\theta(t) = \Delta\theta'_p \exp(-t/t'_\infty)$, where $\Delta\theta'_p$ reflects the disk's orientation when the laser is blocked. From both fits, the excitation and relaxation times agree well, $t_\infty = t'_\infty = 1.1 \pm 0.5$ s. The same disk has been subjected to a series of step-stress measurements from lowest to highest laser power: 0.27 W $\leq P \leq$ 1.5 W (Fig. 3). For all P, the three-parameter model provides a reasonable fit. At low P, $\Delta\theta_p$ increases linearly with P. We find that t_∞ and t_0 are essentially independent of P; averaging over all P yields mean values of $\bar{t}_\infty = 1.2 \pm 0.3$ s and $\bar{t}_0 = 51 \pm 9$ s.

The bulk rheology of gelatin depends strongly on its shear history. Gelatin allowed to "set" in a rheometer exhibits strain stiffening followed by yielding [21,22], as we have verified. However, gelatin subjected to a moderate preshear during loading exhibits only yielding behavior. In the process of initially aligning the disk, we locally preshear the gelatin around it, so we compare the microrheological response with the macroscopic measurements of presheared gelatin. Through this comparison, we seek the geometrical factors required to determine the effective stress and strain around a microdisk subjected to an optical torque. Dimensionally, the shear stress τ applied by the rigid disk to the surrounding polymer network is $\tau \approx T/V$, where V is a characteristic volume, the precise value of which, while theoretically unknown, we expect to be near the spherical volume swept out by the rotating microdisk, $4\pi a^3/3 \approx 14$ μm^3. Deducing the shear strain, γ, from the rotation of the disk is more difficult, since the strain could depend on distance in the gelatin away from the disk. To a first approximation, it is reasonable to assume that the effective shear strain near the disk is proportional to $\Delta\theta$, recognizing that the precise strain field cannot be determined without advanced knowledge of the extensional and shear response of the polymer solution.

Given these limitations, in Fig. 4 we coplot $T(\Delta\theta_p)$ from the optical microrheology measurement together with $\tau(\gamma)$ obtained macroscopically and extract an empirical value for V as well as the connection between $\Delta\theta_p$ and γ. The relative scales of the two horizontal axes and the two vertical axes have been adjusted to provide the best overlap of the data at low and high stresses. At low $T < 3.0 \times 10^{-10}$ dyn cm, $\Delta\theta_p$ increases proportionally with the applied T, and the microrheological response can be fit to a straight line. At the highest $T \approx 3.9 \times 10^{-10}$ dyn cm the resulting $\Delta\theta_p$ is significantly greater than the line extended from lower T, indicating that the gelatin network is responding in a nonlinear manner by yielding. While strictly speaking, the modified Kelvin-Voigt model is valid only in the linear regime, the deviation

from linearity at the highest T is significantly greater than the uncertainty in $\Delta\theta_p$, approximately the symbol size (± 0.03 rad), and the onset of nonlinearity is quite clear. This yielding at the highest P can be attributed to local stress-induced weakening of the gelatin network due to the optical torque exerted by the disk. Correspondingly, the macroscopic rheology exhibits a linear region followed by yielding, $\tau_y \approx 15 \pm 3$ dyn/cm^2. Clearly, as the applied stress exceeds the yield stress and approaches 19 dyn/cm^2, the departure from linearity is substantial. At these higher stresses and strains, the gelatin network is no longer able to maintain a linear response and yields, as some of the strong entanglements in the gel release when the polymers become significantly stretched. While there is no inherent reason to expect universal accordance between microscopic and macroscopic behavior for all soft materials at all concentrations, for this presheared gelatin sample, the shape of the microscopic torque-angle relationship is very similar to the shape of the macroscopic stress-strain relationship. As such, we extract a value for $V \approx 21$ μm^3, equal to approximately 150% of the volume swept out by the rotating microdisk. Moreover, from the good overlap between the microscopic and macroscopic curves, we deduce the effective microscopic strain: $\gamma \approx (0.3 \text{ rad})^{-1}\, \Delta\theta_p$.

In summary, by controlling optical stresses applied by a solid microdisk in a gelatin network, we have measured the local nonlinear microrheological behavior of a soft material. Through a series of step-stress measurements induced by a rotating wax microdisk and a calibration in a simple viscous liquid, we have measured the microscopic yielding of the material. The shape of the torque-angle relationship compares well with the stress-strain relationship obtained from macroscopic mechanical rheometry, providing a means to extract an empirical value for V, and indicating that shear stresses play an important role, even if osmotic compressional stresses in the gelatin could contribute to the disk's response. This value of V and the relationship between $\Delta\theta_p$ and γ can be tested theoretically and experimentally through the measurement of microscopic yield stresses. The generality of the correspondence between microscopic and macroscopic nonlinear behavior for a wide range of soft materials having $\xi \ll a$, if it exists, remains to be shown. To better understand our results, as well as the limitation of this correspondence, an accurate calculation of the evolving shear and extensional strain field, as well as the local osmotic compression of the network, around a rotating disk in dispersed elastic material with a yield stress and a low frequency relaxation is needed. Smaller microdisks having the same aspect ratio, yet with thicknesses larger than the diffraction-limited beam waist, could provide access to local τ approaching 10^2 dyn/cm^2 at $P \approx 1$ W. At higher $P \approx 10$ W, one can potentially measure yield stresses that range up to 10^3 dyn/cm^2. At such large P, only nonabsorbing probes and nonabsorbing soft materials that minimally scatter light would be suitable. As we have demonstrated here, some important soft biomaterials, such as gelatin, fit these constraints. It is conceivable that quantitative nonlinear torque response measurements could even be conducted *in vivo* inside cells.

We thank Jung-Ren Huang for stimulating discussions and programming assistance and the ACS PRF Grant No. 42858-AC7 for financial support.

[1] R. G. Larson, *The Structure and Rheology of Complex Fluids* (Oxford, New York, 1999).
[2] W. M. Gelbart and A. Ben-Shaul, J. Phys. Chem. **100**, 13169 (1996).
[3] T. G. Mason and D. A. Weitz, Phys. Rev. Lett. **74**, 1250 (1995).
[4] T. G. Mason, K. Ganesan, J. H. van Zanten, D. Wirtz, and S. C. Kuo, Phys. Rev. Lett. **79**, 3282 (1997).
[5] P. A. Valberg and H. A. Feldman, Biophys. J. **52**, 551 (1987).
[6] F. Amblard, A. C. Maggs, B. Yurke, A. N. Pargellis, and S. Leibler, Phys. Rev. Lett. **77**, 4470 (1996).
[7] A. R. Baush, W. Moller, and E. Sackmann, Biophys. J. **76**, 573 (1999).
[8] G. Holzwarth, K. Bonin, and D. B. Hill, Biophys. J. **82**, 1784 (2002).
[9] T. M. Squires and J. F. Brady, Phys. Fluids **17**, 073101 (2005).
[10] N. Cappallo, C. Lapointe, D. H. Reich, and R. L. Leheny, Phys. Rev. E **76**, 031505 (2007).
[11] P. Habdas, D. Schaar, A. C. Levitt, and E. R. Weeks, Europhys. Lett. **67**, 477 (2004).
[12] A. Meyer, A. Marshall, B. G. Bush, and E. M. Furst, J. Rheol. **50**, 77 (2006).
[13] Z. Cheng, P. M. Chaikin, and T. G. Mason, Phys. Rev. Lett. **89**, 108303 (2002).
[14] S. B. Ross-Murphy, Polymer **33**, 2622 (1992).
[15] M. Shibayama and M. Okamoto, J. Chem. Phys. **115**, 4285 (2001).
[16] M. Djabourov, Contemp. Phys. **29**, 273 (1988).
[17] A. Ashkin, J. M. Dziedzic, J. E. Bjorkholm, and S. Chu, Opt. Lett. **11**, 288 (1986).
[18] M. P. Sheetz, *Laser Tweezers in Cell Biology* (Academic, San Diego, 1998).
[19] Z. Cheng and T. G. Mason, Phys. Rev. Lett. **90**, 018304 (2003).
[20] A. Davis and H. Stone, Q. J. Mech. Appl. Math. **51**, 495 (1998).
[21] R. D. Groot, A. Bot, and W. G. M. Agterof, J. Chem. Phys. **104**, 9202 (1996).
[22] C. Storm, J. J. Pastore, F. C. MacKintosh, T. C. Lubensky, and P. A. Janmey, Nature (London) **435**, 191 (2005).